Biochimica et Biophysica Acta 1847 (2015) 690–697

Contents lists available at ScienceDirect

Biochimica et Biophysica Acta

journal homepage: www.elsevier.com/locate/bbabio

Role of subunit III and its lipids in the molecular mechanism of cytochrome *c* oxidase

Vivek Sharma [a,*], Pauliina Ala-Vannesluoma [a], Ilpo Vattulainen [a,b], Mårten Wikström [c], Tomasz Róg [a]

[a] Department of Physics, Tampere University of Technology, FI-33101 Tampere, Finland
[b] MEMPHYS, Center for Biomembrane Physics, Department of Physics, University of Southern Denmark, Odense, Denmark
[c] Helsinki Bioenergetics Group, Programme for Structural Biology and Biophysics, Institute of Biotechnology, University of Helsinki, FI-00014 Helsinki, Finland

ARTICLE INFO

Article history:
Received 2 February 2015
Received in revised form 7 April 2015
Accepted 12 April 2015
Available online 17 April 2015

Keywords:
Molecular dynamics simulation
Continuum electrostatic
Water molecule
Oxygen diffusion
Cardiolipin

ABSTRACT

The terminal respiratory enzyme cytochrome *c* oxidase (C*c*O) reduces molecular oxygen to water, and pumps protons across the inner mitochondrial membrane, or the plasma membrane of bacteria. A two-subunit C*c*O harbors all the elements necessary for oxygen reduction and proton pumping. However, it rapidly undergoes turnover-induced irreversible damage, which is effectively prevented by the presence of subunit III and its tightly bound lipids. We have performed classical atomistic molecular dynamics (MD) simulations on a three-subunit C*c*O, which show the formation of water wires between the polar head groups of lipid molecules bound to subunit III and the proton uptake site Asp91 (*Bos taurus* enzyme numbering). Continuum electrostatic calculations suggest that these lipids directly influence the proton affinity of Asp91 by 1–2 p*K* units. We surmise that lipids bound to subunit III influence the rate of proton uptake through the D-pathway, and therefore play a key role in preventing turnover-induced inactivation. Atomistic MD simulations show that subunit III is rapidly hydrated in the absence of internally bound lipids, which is likely to affect the rate of O_2 diffusion into the active-site. The role of subunit III with its indigenous lipids in the molecular mechanism of C*c*O is discussed.

© 2015 Elsevier B.V. All rights reserved.

1. Introduction

The respiratory chains of mitochondria and many bacteria terminate in cytochrome *c* oxidase (C*c*O), which catalyzes the reduction of molecular oxygen to water, and couples the free energy of the reaction to proton pumping across the membrane [1–3]. The oxygen reduction reaction catalyzed by C*c*O is spectacular in the sense that it proceeds without any production of toxic reactive oxygen species. The electrons and protons required for oxygen reduction are supplied from the P- and N-side of the membrane, respectively, which leads to the generation of an electrical gradient across the membrane [2,3]. The concurrent translocation of protons from the N-side to the P-side further contributes to the established proton electrochemical gradient (or proton motive force — *pmf*) [1]. The *pmf* is then utilized by the ATP-synthase to generate ATP from ADP and inorganic phosphate (P_i) [2,3].

The structures of most of the intermediates of the catalytic cycle of C*c*O are known [3,4]. The thermodynamics and kinetics pertaining to elementary electron/proton transfer steps are also well understood [3,4]. Several high resolution crystal structures of C*c*O in different redox states are available [5–9], which together with site-directed mutagenesis studies have assisted in the identification of proton transfer pathways buried deep within the enzyme [10,11].

Overall, C*c*Os are classified into three subtypes: A, B, and C [12]. The three largest membrane-bound subunits (I–III) are highly conserved in the A-type mitochondrial and bacterial oxidases. Subunits I and II harbor all the necessary components that are required to catalyze oxygen reduction and proton pumping, whereas the role of subunit III, which does not contain any redox centers or known proton-conducting pathways, remains less clear. However, it is well established that subunit III provides additional stability to the enzyme while it undergoes turnover [13–15]. The catalytic activity of a two-subunit enzyme at pH = 8 is about 10–100 fold lower than when subunit III is present [15]. In contrast, at pH 6.5 and below, a two-subunit enzyme displays near wild-type activity [15]. This suggests that the presence of subunit III is critical for enzymatic activity, especially at high pH. An additional consequence of the absence of subunit III is that the enzyme rapidly undergoes turnover-induced inactivation (also called 'suicide inactivation'), by which it is irreversibly damaged [13,14]. The molecular mechanism of this turnover-induced impairment is not clear, and various possibilities such as slower rate of proton transfer via the D-pathway, and/or subsequent destabilization of the active-site, or loss of Cu_B, have been proposed [14,16]. Indeed, the N-terminal segment of subunit III houses

Abbreviations: MD, molecular dynamics; PE, phosphatidylethanolamine; PC, phosphatidylcholine; CL, cardiolipin; C*c*O, cytochrome *c* oxidase.

* Corresponding author at: Department of Physics, Tampere University of Technology, PO Box 692, FI-33101 Tampere, Finland. Tel.: +358 50 5759509.
E-mail address: vivek.sharma@tut.fi (V. Sharma).

http://dx.doi.org/10.1016/j.bbabio.2015.04.007
0005-2728/© 2015 Elsevier B.V. All rights reserved.

histidine residues that may form a proton-buffering region, in the absence of which a slower rate of proton transfer via the D-pathway can be expected [17].

Lipids are known to play important roles in the molecular mechanism of many membrane proteins [18–20]. In the case of inner-mitochondrial membrane proteins, cardiolipins constitute the most studied and discussed lipid group [21]. It is therefore not surprising that the crystal structures of many membrane proteins have revealed tightly bound cardiolipin molecules [18,22]. Indeed, mitochondrial C*c*O is known to bind cardiolipin molecules together with other phospholipids [22,23]. The alteration of some of these lipid binding-sites destabilizes inter-subunit interactions, and also affects the catalysis [24]. Both coarse-grained and atomistic molecular dynamics (MD) simulations have assisted in highlighting the importance of cardiolipin–protein interactions in C*c*O, as well as in the cytochrome bc_1 complex [25–27].

In this study, we concentrate on the function of lipid molecules tightly bound in the V-shaped cleft formed by two clusters of transmembrane helices of subunit III [5–7,28,29] (Fig. 1). X-ray structures from different organisms show that phosphatidyl glycerol (PG), phosphatidyl ethanolamine (PE), and phosphatidyl choline (PC) lipids are found at this location [5–7,28,29]. The lipid molecules are stabilized through conserved electrostatic and hydrophobic contacts within the protein structure [22,30]. Based on X-ray structure analysis and site-directed mutagenesis studies, it has been proposed that the hydrophobic interior of subunit III forms a local reservoir for O_2, and the entrance to an O_2 diffusion pathway from the membrane into the active-site [31].

1.1. Rationale

Based on the observations that subunit III binds two lipid molecules, and any alteration of the lipid binding site results in a phenotype similar to a subunit III-deficient enzyme (suicide inactivation) [30], we hypothesize that the lipid molecules of subunit III may play an important role in channeling the protons towards Asp91, which may modulate the rate of proton transfer in the D-pathway. These viewpoints are tested here by computational methodology.

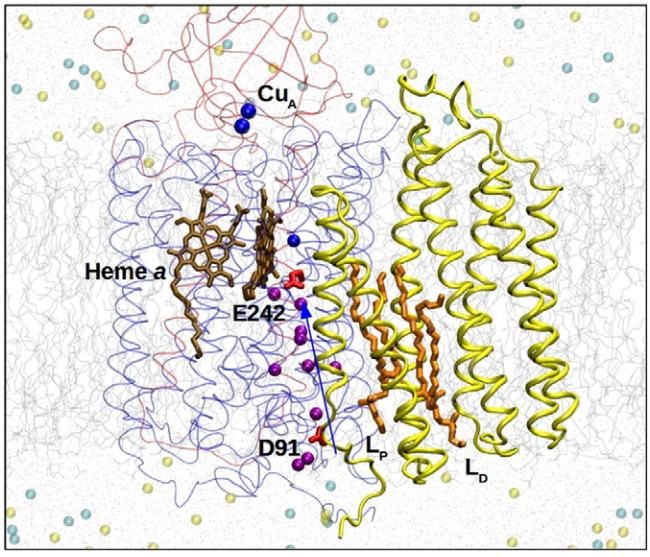

Fig. 1. Structure of C*c*O in a membrane-solvent environment. Subunits I (blue), II (red), and III (yellow/thicker) are shown as ribbons. Hemes, copper atoms, and subunit III bound lipids are shown in brown, blue, and orange, respectively. Lipids proximal (L_P) and distal (L_D) to the proton-uptake site (D91, in red) are marked. The D-pathway (blue arrow) terminates at a highly conserved residue near the active-site (E242, shown in red). Crystallographic water molecules present in the D-pathway, and Na^+ and Cl^- ions are shown as purple, blue, and yellow spheres, respectively.

2. Computational methods

2.1. MD simulations

Classical MD simulations were performed on a three-subunit C*c*O (PDB id 1V54 [5]) immersed in a hybrid lipid bilayer comprising DLiPC (1,2-dilinoleyl-sn-glycero-3-phosphatidylcholine), DLiPE (1,2-dilinoleyl-sn-glycero-3-phosphoethanolamine) and CL (4-linoleic cardiolipin) molecules (Fig. 1). The ratio of CL:DLiPC:DLiPE molecules in the system was 1:3.38:3.05, in agreement with our earlier studies [27,32]. The membrane-protein system was solvated with TIP3 water molecules, and Na^+ and Cl^- ions. The conserved lipid binding site in subunit III was modeled with or without lipids. Different types of lipids were modeled at the site; 1 CL, 2 PG or 2 PE molecules (Table 1). The model system comprised ca. 280,000 atoms. All amino acid residues were considered in their standard protonation states, except functionally critical residues for which protonation states are known from experimental data [3,32]. Glu242, Asp364 and Lys319 from subunit I were protonated, whereas Tyr244 was deprotonated (see below in this Section 2.1). 20 to 150 ns MD runs were performed on the constructed model systems. The NAMD [33] program was used to perform the simulations using the CHARMM [34] force field. The charges and parameters of metal centers were obtained from Johansson et al. [35]. In all simulations, the low-spin heme was reduced and the binuclear center was in the P_M state (ferryl heme a_3, cupric Cu_B with a fourth OH^- ligand, and Tyr244 as the neutral radical). Simulation parameters were T = 310 K for temperature, $p = 1$ atm for pressure, 1 fs for the timestep, and particle mesh Ewald (PME) used for computing electrostatic interactions [36]. Total time comprising all simulations was ~0.78 μs. Analysis of simulation trajectories was done with the help of the VMD program [37].

2.2. Continuum electrostatic calculations

The electrostatic calculations were performed on snapshots obtained from MD simulations. A total of 50 snapshots were taken from individual simulation trajectories. The MEAD package [38,39] was used to solve the linearized Poisson–Boltzmann equation. The intrinsic pK_as and site–site interaction energy data from MEAD calculations were used in the KARLSBERG [40,41] program to estimate the final pK_a. The p$K_{a,model}$ of Asp, Glu, Arg, Lys, Tyr and His was 4.5, 4.6, 12.0, 10.4, 9.6 and 6.2, respectively. The propionate groups of hemes, and the oxygenous ligand of Cu_B were also treated as titratable groups with p$K_{a,model}$ of 4.8 and 9.5, respectively.

3. Results

3.1. Proton funneling groups

We surmise that the headgroups of the lipids bound to subunit III might play an important role in channeling the protons towards Asp91 at the entrance of the D-pathway. Such information is not evident

Table 1
Simulation setup and time.

Simulation	Type of lipid modeled in su III	Time (ns)
1	No lipid (run I)	150
2	No lipid (run II)	150
3	2 PE molecules	100
4	2 PG molecules	50
5	1 CL molecule	100
6	2 PE molecules[a]	100
7	2 PE molecules/Asp91 protonated	60
8	2 PE molecules/Asp91Asn mutant	50
9	No lipid/Asp91Asn mutant	20

[a] Lipid binding site mutants; R96A in subunit I, and R221A, W58A and F86A in subunit III.

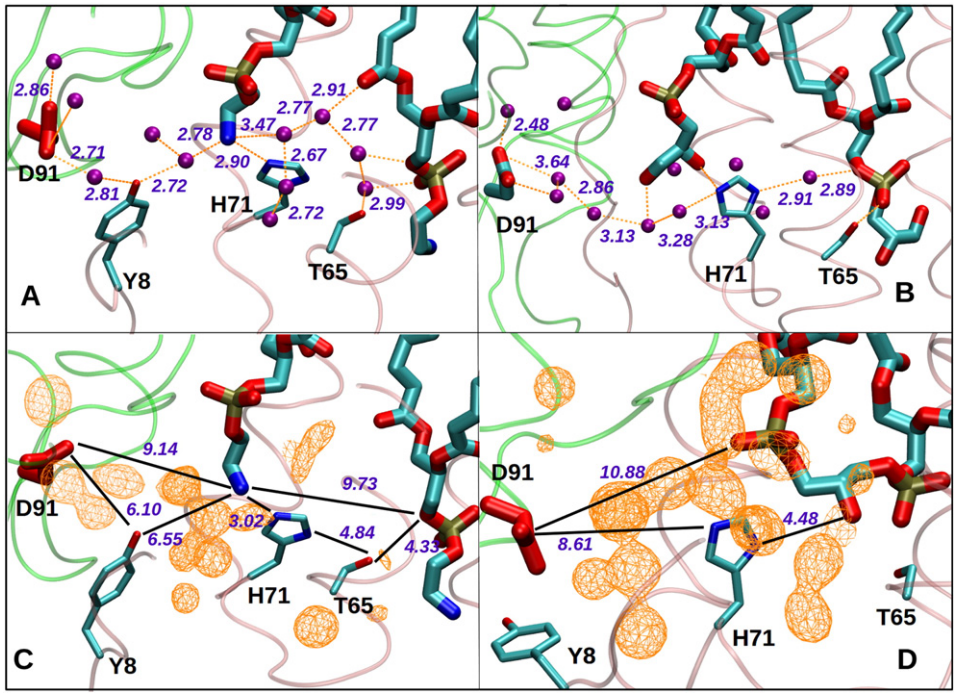

Fig. 2. A) and B) Snapshots from simulations showing a water wire between the proton uptake site, Asp91, and the lipid headgroups (PE and PG molecules in panels A and B, respectively). C) and D) Occupancy of water molecules displayed as orange wireframe (isovalue = 0.4). Occupancy is calculated over the entire simulation trajectory (PE and CL molecules in panels C and D, respectively). Water molecules (in purple with no hydrogen atoms attached), and polar amino acid residues from subunit III, Tyr8, Thr65, and His71 are also shown. The marked distances are in ångströms.

from the analysis of static crystal structures, but the dynamic data from simulations show that transient water wires form between the polar head group region of lipids and Asp91 (Fig. 2A and B). The identities of the water molecules participating in water wire formation change during the simulations. However, water occupancy data suggest that a water-mediated connection remains persistent throughout the trajectory (Fig. 2C and D). The water wires connecting Asp91 with the lipid headgroups are also stabilized by the sidechains of polar amino acid residues from subunit III, as shown in Fig. 2A and B.

The data presented in Fig. 3 displays that regardless of the type of lipid modeled in subunit III, the lipid–protein hydrogen bonding interactions observed in the crystal structure remain stable. The conserved arginines (96 and 221 from subunits I and III, respectively) form ionic interactions with the charged lipid head groups that remain stable throughout the trajectory (Fig. 3). In addition, stable hydrogen bonds are also formed between the lipid head groups and the backbone or sidechain of amino acid residues (see Fig. 3). In agreement with the crystal structure data [22], the analyses suggest that the lipids are strongly bound to subunit III.

In the case when simulations are performed without subunit III-bound lipids (two independent simulations, see Table 1), structural perturbations take place; the loop between helices II and III of subunit III undergoes a large conformational change bringing two histidine residues (His70 and His71) away from their crystallographic positions (Fig. 4). The same data is presented as root mean square fluctuation (rmsf) of the entire loop segment between helices II and III in different simulation conditions (Fig. 5). In the case when lipids are bound to subunit III, the segment's rmsf remains low, whereas it increases when subunit III is lipid-deficient. A similar observation is also made in an independent 100 ns simulation in which lipid-binding site mutants (Table 1; Ref. [30]) were created in-silico (Fig. 5). This suggests that the mobility of lipids bound to subunit III is important for the structural stability of the loop segment.

The histidine residues are known to act as localized proton buffers in many membrane proteins (pK_a^{His} ~ pH of the solution), and assist in relaying protons towards the proton-uptake sites [42–44]. The structural perturbation of the loop segment, which comprises two histidine residues (His70 and His71), is likely to alter the relay of protons towards Asp91 from the latter residues. Indeed, unfolding of the latter segment causes histidine residues to distance from Asp91 (Fig. 4), whereas both of these residues approach each other transiently ($d_{H71-D91}$ ~ 8–10 Å, see Fig. 2D) in bound-lipid simulations.

Among the two histdines, His71 is highly conserved, and is sandwiched between the two lipid headgroups. In simulations it is observed to attain multiple conformations (Fig. 2). It constantly participates in either direct or water-mediated hydrogen bonding (H-bonding) with the lipid molecules (a direct hydrogen bond in ca. 15–40% of simulation time). In addition, His71 stabilizes water wires towards Asp91, thereby providing a connection between the bulk and the proton uptake site (Fig. 2). This suggests that His71 can acquire multiple roles such as being a transient proton reservoir, or channeling bulk protons towards Asp91. The high degree of conservation together with its unique location makes His71 a potential site for biochemical testing.

3.2. The lipid headgroups modulate the pK_a of Asp91

In order to test if the lipids in subunit III perturb the pK_a of Asp91, we performed continuum electrostatic calculations on snapshots obtained from the MD simulations. The results show that the subunit III lipids induce a significant increase in the pK_a of Asp91. Depending upon the type of lipid, the proton affinity of Asp91 increases by as much as 2 pK units. Since the population of the protonated form of Asp91 is likely to control the rate of proton transfer through the D-pathway, the subunit III lipids may indeed contribute to this proton transfer (see Section 4).

3.3. Hydration of the lipid binding site

Two independent MD simulations show that in the absence of internal lipids, the V-shaped cleft of subunit III is rapidly filled with water molecules (Fig. 6). The water molecules enter the region primarily from the N-side of the membrane, and reach up to the level where the lipid tails would reside (Fig. 7), thereby hydrating the region

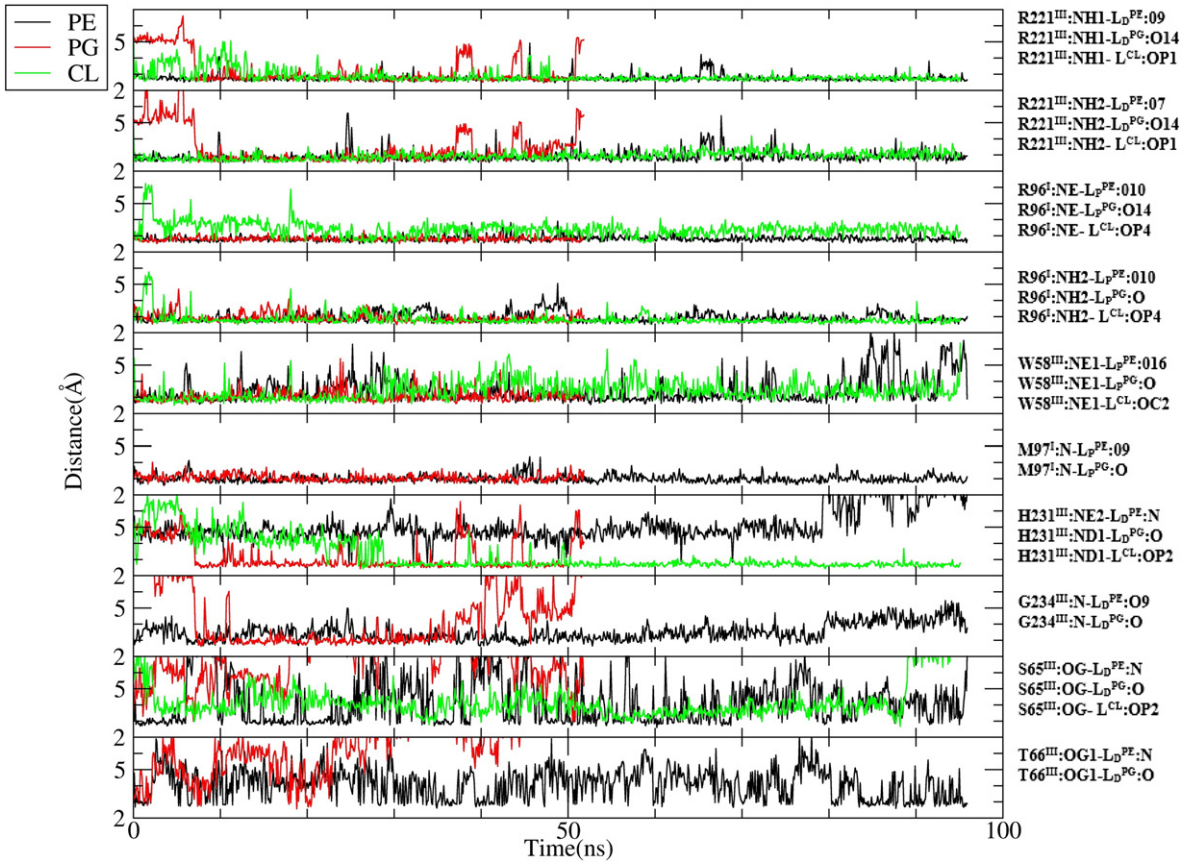

Fig. 3. Stability of lipid–protein interactions. The hydrogen bonds between the subunit III bound lipid head groups and amino acid residues [see Ref. 22] are plotted as distance versus simulation time.

considerably. Extensive hydration of this domain, which is thought to form the entrance to the O_2 diffusion pathway [31], might impede the diffusion of molecular oxygen towards the active site (Fig. 7), which may in turn result in an increase in apparent K_M for O_2 (see Section 4). By contrast, no water penetration takes place when simulations are performed with lipids bound to subunit III (Fig. 6), which is most likely due to the tighter packing of the lipid tails (Fig. 7). The hydrophobic packing at this site is also supplemented by the tails of a lipid molecule that binds at the surface of subunit III (see Fig. 7), in a conformation completely consistent with the crystal structure data [22].

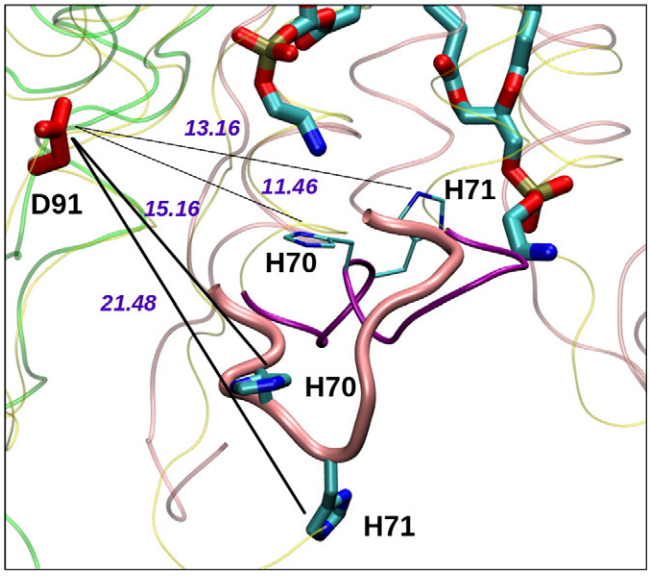

Fig. 4. Unfolding of the segment between helices II and III in the absence of subunit III-bound lipids (thick/pink). The segment remains close to its crystallographic conformation (thin/purple) in the simulations when lipids are bound to subunit III (2 PE molecules shown). Note the departure of two histidines from their crystallographic positions (His70 and His71 in thicker representations). Distances shown are in ångströms.

4. Discussion

In many proton-translocating membrane proteins, acidic residues such as glutamates and aspartates form a cluster around the proton

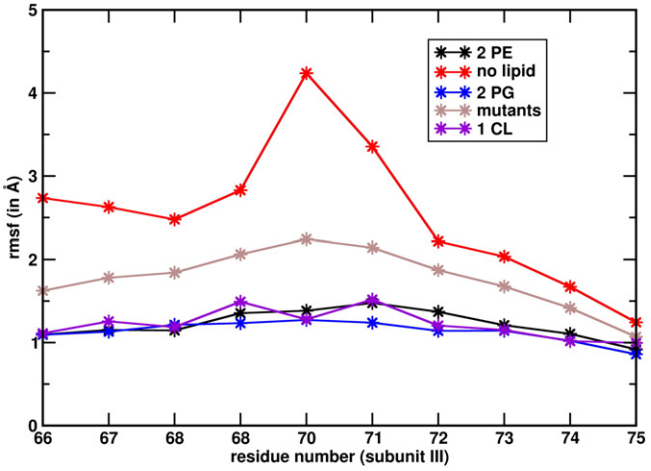

Fig. 5. Root mean square fluctuation (rmsf) of the loop segment (residues # 66–75) in subunit III, in different simulation conditions. In-silico mutations are; R96A in subunit I, and R221A, W58A and F86A in subunit III.

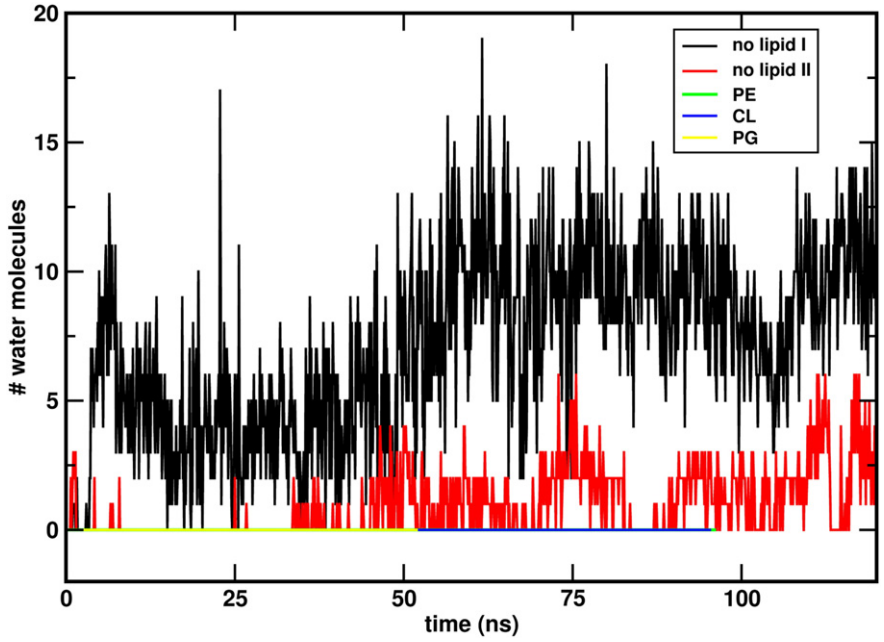

Fig. 6. Number of water molecules in subunit III cleft region in different simulation conditions.

uptake site and assist in funneling the protons towards the latter [42–44]. A similar proton-collecting antenna function has also been assigned to the phospholipid molecules [45–47]. With their charged headgroups, the phospholipids create a zone of negative potential, which attracts bulk protons towards the membrane–water interface [46]. The histidine residues located on the protein surface, in turn, act as localized proton buffers because their pK_a lies close to the pH of the medium. If there are protonic connections between the proton-collecting antenna region and the proton-uptake site, such an arrangement is likely to enhance the rate of proton transfer between the two [46].

Subunit III of CcO tightly binds two phospholipids (Fig. 1). Due to the proximity of the head group of the lipid closest to the proton uptake site Asp91 (d_{Lp-D91} ~ 10 Å, Figs. 1 and 2), it can be conjectured that either one or both lipids attract protons, and assist them in channeling towards the D-pathway opening at Asp91. In agreement with this, the X-ray data show that the lipid distal to Asp91 has its head group much more surface exposed, which may indeed help in attracting bulk protons (see also Figs. 1 and 2). The water wires, stabilized by the assistance of lipid headgroups and proteinaceous residues (Fig. 2), provide the required protonic connectivity between the proton-buffers such as histidines (e.g. His71) and the proton-uptake site Asp91 (Fig. 2). However, in the case when the subunit III lipids are missing, the perturbations in protein structure (Fig. 4) are likely to make proton transfer towards Asp91 more difficult.

The pK_as of the phosphate groups of lipids are generally low, and they are likely to remain deprotonated at physiological pH [48]. However, the situation is different with CL, which has two titratable sites, and has been shown to undergo protonation coupled with a conformational change [49,50]. If a scenario is envisaged in which the subunit III cleft binds a single CL molecule (compared to 2 PG or 2 PE molecules), the latter could act as a potential proton reservoir and aid in rapid proton supply to the D-pathway through intervening water molecules (Fig. 2D). Alternatively, a negatively charged CL molecule may attract protons, but His71 could be the actual proton reservoir and/or donor to Asp91. The simulation data indeed show that the two residues approach each other ($d_{min(H71-D91)}$ ~ 8 Å), and are connected by a water wire (Fig. 2).

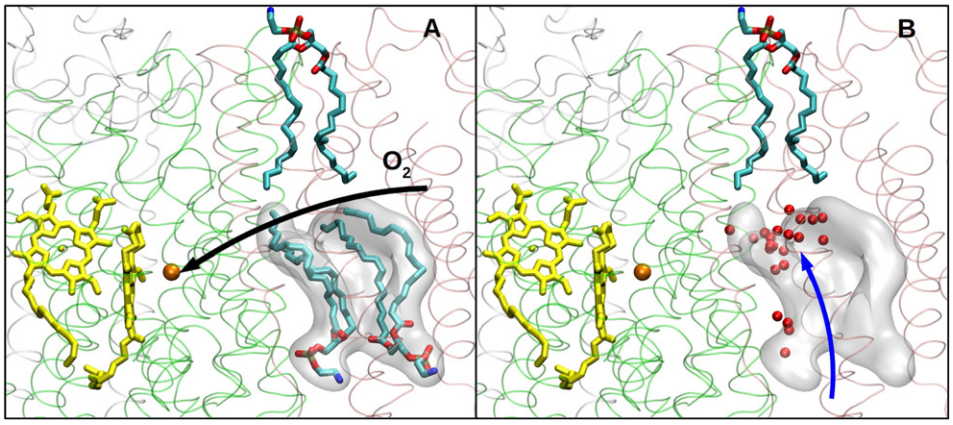

Fig. 7. A) O_2 diffusion pathway through the subunit III cleft. B) Water molecules (red spheres) enter the subunit III cleft in the absence of lipids (blue arrow). Subunits I, II, and III are displayed as green, white, and pink ribbons, respectively. Hemes (yellow) and Cu_B (orange) are also shown.

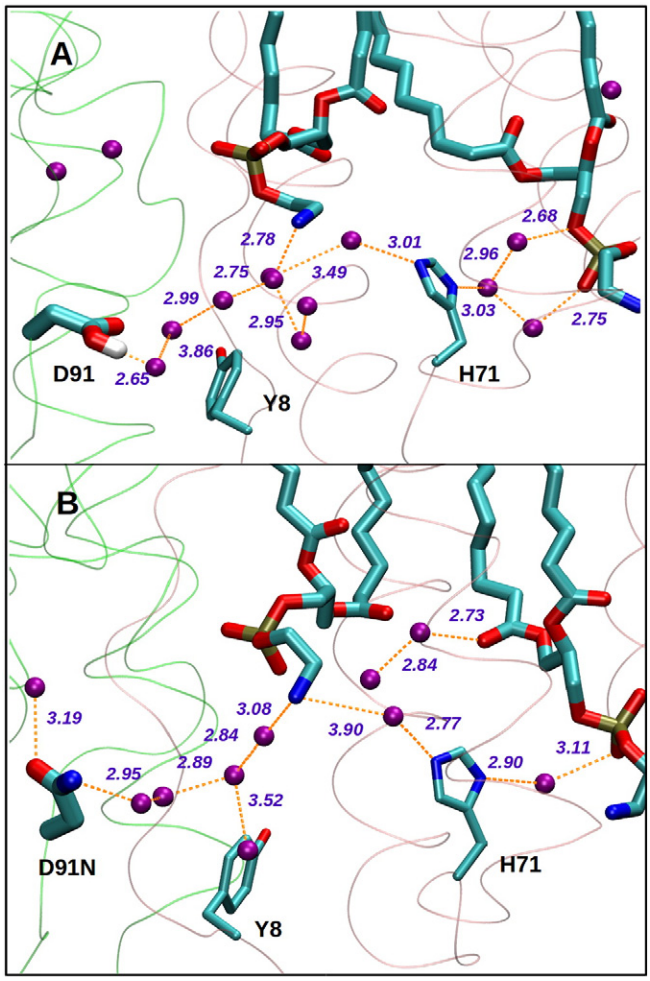

Fig. 8. Simulation snapshots showing water wire between the phospholipid (2 PE molecules) head groups and protonated Asp91 (A) and Asp91Asn mutant (B). Distances shown are in ångströms.

Overall, the data supports the viewpoint that a CL molecule may bind with subunit III in a stable manner (Fig. 3), and enhance the rate of proton transfer towards Asp91. However, a CL molecule has never been observed in any of the crystal structures of A-type oxidases [5–7,28,29], which could be due to the specific protocols used for purification and crystallization. Nevertheless, in agreement with our hypothesis, recent work has indeed concluded that a CL molecule could bind in the subunit III cleft, and modulate enzymatic activity [51].

Continuum electrostatic calculations suggest that the lipid molecules increase the proton affinity of Asp91 by 1–2 pK units. This increase is likely to enhance the rate of proton transfer in the D-channel by 10 to 100 fold given the relationship,

$$v = k[\mathrm{AH}],$$

where k is the proton transfer rate constant, and [AH] is the concentration of protonated Asp91 [52].

For a proton to be transferred from the N-side of the membrane to the active site via the D-pathway, transient protonation of Asp91 is likely to occur. Therefore, in order to test if the observed water wires between the lipid head groups and Asp91 (Fig. 2) still persist when the latter is protonated, we performed an additional simulation (Table 1). As shown in Fig. 8, analogous water wires form even when Asp91 is protonated. However, the water structure immediately around it is perturbed, which suggests that the deprotonated form of Asp91 stabilizes a much stronger H-bond with the water molecules around it than the protonated form (Fig. 9).

Overall, based on computational predictions, we hypothesize that the lipid molecules present in subunit III play an important role in maintaining rapid proton uptake through the D-channel both by increasing the proton affinity of Asp91, and by sustaining water-wires towards it. The experimentally observed increased propensity of suicide inactivation upon alteration of lipid binding site is therefore probably due to the slower rate of proton transfer towards Asp91 (perturbed protein–water structure), and in the D-pathway itself (lower pK_a of Asp91) (see also Ref. [16]).

Previous experimental data showed that in addition to the lipid binding site mutants, the Asp (Asp132 in *Rhodobacter sphaeroides*) → Asn mutation results in further increase in the tendency

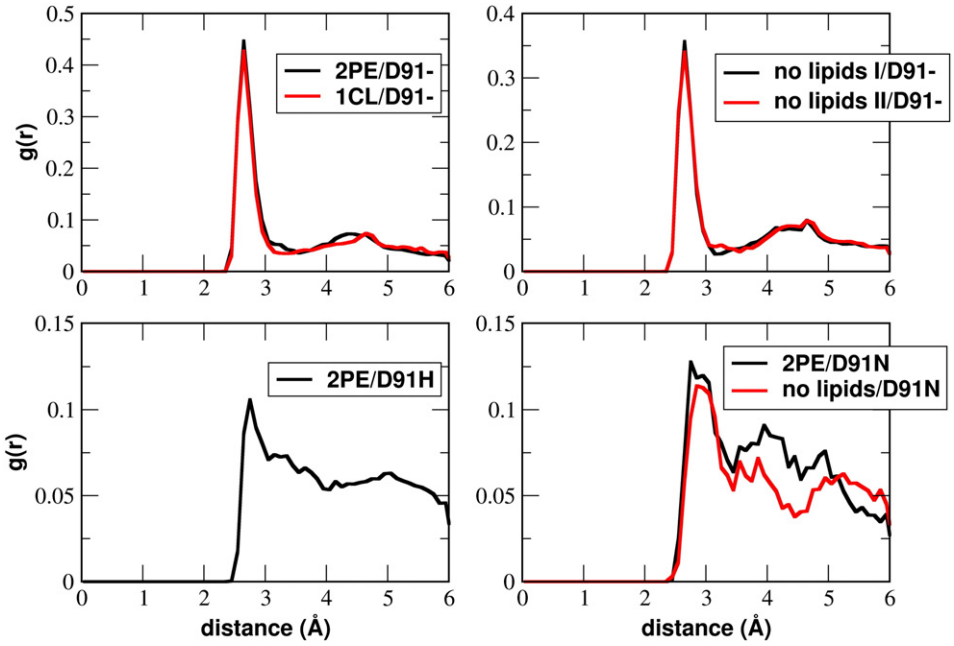

Fig. 9. Radial distribution functions showing water structure around deprotonated (D91-) and protonated (D91H) Asp91, and Asp91Asn mutant (D91N), calculated from with – (2 PE or 1 CL molecule) and without – (no lipids) lipid simulations.

of suicide inactivation [30]. On the basis that lipid-binding site mutants cannot cause a more drastic effect than the severe D-pathway Asp/Asn mutant itself, it was suggested that it is not the slow proton transfer through the D-channel that causes suicide inactivation in the lipid binding site mutants, but the structural perturbations at the subunit I/III interface or at the active site are the actual cause of the effect [30]. However, we provide an alternative explanation here. Even though the Asp/Asn mutant severely inhibits the proton transfer through the D-pathway, there is nevertheless a residual enzymatic activity (= turnover) [53]. Due to the perturbed lipid–protein–water structure (Figs. 4 and 5), the rate of proton transfer towards the D-pathway opening (Asn now) would further slow down, and would cause the turnover-induced suicide inactivation to set-in in the lipid binding-site mutants.

The Asp/Asn mutation strongly affects the proton transfer activity through the D-pathway [53,54]. The loss of a protonatable site seems to be the primary cause of loss of proton pumping [53,54]. In order to see how the water structure is perturbed when Asp91 is replaced by asparagine, we constructed an in-silico Asp91Asn mutant (Table 1). The data shows that despite the stable water wires between the lipid head groups and asparagine (Fig. 8B), the hydrogen bonding interactions between the latter and the water molecules are strongly perturbed (Fig. 9), which may contribute to a diminished proton transfer activity through this route.

In addition to the rapid access to protons, the active site of oxidase also needs rapid supply of the substrate O_2. The V-shaped cleft in subunit III has been suggested to form a reservoir and an opening of an O_2 diffusion channel from the membrane to the binuclear site [31]. The cleft is ideally located for this purpose, and is highly hydrophobic due to the presence of non-polar amino acid residues and the lipid tails (Figs. 1 and 7). The simulation data presented here show that when the lipid molecules from subunit III are removed, the vacancy is rapidly filled by water molecules. This hydration coincides with the region in which O_2 molecules would transiently reside or diffuse through, and, is therefore, likely to hinder its diffusion towards the active-site.

It has been reported that the binding affinity (K_D) of ligands such as azide and cyanide remains unaffected upon lipid removal from subunit III [51]. Although a similar scenario can be envisaged for the substrate O_2, we propose that the hydration of cleft in the subunit III structure could lower the local O_2 concentration, and slow down O_2 diffusion. Such an effect may increase the apparent K_M for oxygen (V_{max} and K_D remain unchanged), a situation akin to an earlier kinetic analysis [31], and open for experimental testing in the future.

Transparency document

The Transparency document associated with this article can be found, in the online version.

Acknowledgements

VS acknowledges postdoctoral researcher funding from the Academy of Finland. Further financial support by the Sigrid Jusélius Foundation (MW, IV), the Academy of Finland Center of Excellence program (VS, PAV, TR, IV), and the European Research Council (Advanced Grant CROWDED-PRO-LIPIDS) (IV) is also acknowledged. We thank CSC — IT Center for Science, Espoo, Finland, for computational resources.

References

[1] M. Wikström, Proton pump coupled to cytochrome *c* oxidase in mitochondria, Nature 266 (1977) 271–273.
[2] S. Ferguson-Miller, G.T. Babcock, Heme/copper terminal oxidases, Chem. Rev. 96 (1996) 2889–2908.
[3] M. Wikström, V. Sharma, V.R.I. Kaila, J.P. Hosler, G. Hummer, New perspectives on proton pumping in cellular respiration, Chem. Rev. 115 (2015) 2196–2221.
[4] M. Wikström, Active site intermediates in the reduction of O_2 by cytochrome oxidase, and their derivatives, Biochim. Biophys. Acta Bioenerg. 1817 (2012) 468–475 (232–240).
[5] T. Tsukihara, K. Shimokata, Y. Katayama, H. Shimada, K. Muramoto, H. Aoyama, M. Mochizuki, K. Shinzawa-Itoh, E. Yamashita, M. Yao, Y. Ishimura, S. Yoshikawa, The low-spin heme of cytochrome *c* oxidase as the driving element of the proton-pumping process, Proc. Natl. Acad. Sci. U. S. A. 100 (2003) 15304–15309.
[6] T. Tsukihara, H. Aoyama, E. Yamashita, T. Tomizaki, H. Yamaguchi, K. Shinzawa-Itoh, R. Nakashima, R. Yaono, S. Yoshikawa, The whole structure of the 13-subunit oxidized cytochrome *c* oxidase at 2.8 Å, Science 272 (1996) 1136–1144.
[7] S. Iwata, C. Ostermeier, B. Ludwig, H. Michel, Structure at 2.8 Å resolution of cytochrome *c* oxidase from *Paracoccus denitrificans*, Nature 376 (1995) 660–669.
[8] J. Abramson, S. Riistama, G. Larsson, A. Jasaitis, M. Svensson-Ek, L. Laakkonen, A. Puustinen, S. Iwata, M. Wikström, The structure of the ubiquinol oxidase from *Escherichia coli* and its ubiquinone binding site, Nat. Struct. Mol. Biol. 7 (2000) 910–917.
[9] T. Tiefenbrunn, W. Liu, Y. Chen, V. Katritch, C.D. Stout, J.A. Fee, V. Cherezov, High resolution structure of the ba_3 cytochrome *c* oxidase from *Thermus thermophilus* in a lipidic environment, PLoS One 6 (2011) e22348.
[10] A.A. Konstantinov, S. Siletsky, D. Mitchell, A. Kaulen, R.B. Gennis, The roles of the two proton input channels in cytochrome *c* oxidase from *Rhodobacter sphaeroides* probed by the effects of site-directed mutations on time-resolved electrogenic intraprotein proton transfer, Proc. Natl. Acad. Sci. U. S. A. 94 (1997) 9085–9090.
[11] M. Wikström, A. Jasaitis, C. Backgren, A. Puustinen, M.I. Verkhovsky, The role of the D- and K-pathways of proton transfer in the function of the haem–copper oxidase, Biochim. Biophys. Acta Bioenerg. 1459 (2000) 514–520.
[12] M.M. Pereira, M. Santana, M. Teixeira, A novel scenario for the evolution of haem–copper oxygen reductases, Biochim. Biophys. Acta Bioenerg. 1505 (2001) 185–208.
[13] M.R. Bratton, M.A. Pressler, J.P. Hosler, Suicide inactivation of cytochrome *c* oxidase: catalytic turnover in the absence of subunit III alters the active site, Biochemistry 38 (1999) 16236–16245.
[14] J.P. Hosler, The influence of subunit III of cytochrome *c* oxidase on the D pathway, the proton exit pathway and mechanism-based inactivation in subunit I, Biochim. Biophys. Acta Bioenerg. 1655 (2004) 332–339.
[15] G. Gilderson, L. Salomonsson, A. Aagaard, J. Gray, P. Brzezinski, J. Hosler, Subunit III of cytochrome *c* oxidase of *Rhodobacter sphaeroides* is required to maintain rapid proton uptake through the D-pathway at physiologic pH, Biochemistry 42 (2003) 7400–7409.
[16] D.A. Milles, J.P. Hosler, Slow proton transfer through the pathways for pumped protons in cytochrome *c* oxidase induces suicide inactivation of the enzyme, Biochemistry 44 (2005) 4656–4666.
[17] K.S. Alnajjar, J. Hosler, L. Prochaska, Role of the N-terminus of subunit III in proton uptake in cytochrome *c* oxidase of *Rhodobacter sphaeroides*, Biochemistry 53 (2014) 496–504.
[18] C. Hunte, Specific protein–lipid interactions in membrane proteins, Biochem. Soc. Trans. 33 (2005) 938–942.
[19] A.W. Smith, Lipid–protein interactions in biological membranes: a dynamic perspective, Biochim. Biophys. Acta Bioenerg. 1818 (2012) 172–177.
[20] P.L. Yeagle, Non-covalent binding of membrane lipids to membrane proteins, Biochim. Biophys. Acta Bioenerg. 1838 (2014) 1548–1559.
[21] G. Paradies, V. Paradies, V. De Benedictis, F.M. Ruggiero, G. Petrosillo, Functional role of cardiolipin in mitochondrial bioenergetics, Biochim. Biophys. Acta Bioenerg. 1837 (2014) 408–417.
[22] K. Shinzawa-Itoh, H. Aoyama, K. Muramoto, H. Terada, T. Kurauchi, Y. Tadehara, A. Yamasaki, T. Sugimura, S. Kurono, K. Tsujimoto, T. Mizushima, E. Yamashita, T. Tsukihara, S. Yoshikawa, Structures and physiological roles of 13 integral lipids of bovine heart cytochrome *c* oxidase, EMBO J. 26 (2007) 1713–1725.
[23] E. Sedlák, M. Panda, M.P. Dale, S.T. Weintraub, N.C. Robinson, Photolabeling of cardiolipin binding subunits within bovine heart cytochrome c oxidase, Biochemistry 45 (2006) 746–754.
[24] E. Sedlák, N.C. Robinson, Phospholipase A(2) digestion of cardiolipin bound to bovine cytochrome *c* oxidase alters both activity and quaternary structure, Biochemistry 38 (1999) 14966–14972.
[25] C. Arnarez, S.-J. Marrink, X. Periole, Identification of cardiolipin binding sites oncytochrome *c* oxidase at the entrance of proton channels, Sci. Rep. 3 (2013) 1263.
[26] C. Arnarez, J.-P. Mazat, J. Elezgaray, S.-J. Marrink, X. Periole, Evidence for cardiolipin binding sites on the membrane-exposed surface of the cytochrome *bc*1, J. Am. Chem. Soc. 135 (2013) 3112–3120.
[27] S. Pöyry, O. Cramariuc, P.A. Postila, K. Kaszuba, M. Sarewicz, A. Osyczka, I. Vattulainen, T. Róg, Atomistic simulations indicate cardiolipin to have an integral role in the structure of the cytochrome *bc*1 complex, Biochim. Biophys. Acta Bioenerg. 1827 (2013) 769–778.
[28] M. Svensson-Ek, J. Abramson, G. Larsson, S. Törnroth, P. Brzezinski, S. Iwata, The X-ray crystal structure of wild-type and EQ(I-286) mutant cytochrome *c* oxidase from *Rhodobacter sphaeroides*, J. Mol. Biol. 321 (2002) 329–339.
[29] A. Harrenga, H. Michel, The cytochrome *c* oxidase from *Paracoccus denitrificans* does not change the metal center ligation upon reduction, J. Biol. Chem. 274 (1999) 33296–33299.
[30] L. Varanasi, D. Mills, A. Murphree, J. Gray, C. Purser, R. Baker, J. Hosler, Altering conserved lipid binding sites in cytochrome *c* oxidase of *Rhodobacter sphaeroides* perturbs the interaction between subunits I and III and promotes suicide inactivation of the enzyme, Biochemistry 45 (2006) 14896–14907.
[31] S. Riistama, A. Puustinen, A. García-Horsman, S. Iwata, H. Michel, M. Wikström, Channelling of dioxygen into the respiratory enzyme, Biochim. Biophys. Acta Bioenerg. 1275 (1996) 1–4.

[32] V. Sharma, G. Enkavi, I. Vattulainen, T. Rog, M. Wikström, Proton-coupled electron transfer and the role of water molecules in proton pumping by cytochrome *c* oxidase, Proc. Natl. Acad. Sci. U. S. A. 112 (2015) 2040–2045.
[33] J.C. Phillips, R. Braun, W. Wang, J. Gumbart, E. Tajkhorshid, E. Villa, C. Chipot, R.D. Skeel, L. Kalé, K. Schulten, Scalable molecular dynamics with NAMD, J. Comput. Chem. 26 (2005) 1781–1802.
[34] A.D. MacKerell, D. Bashford, M. Bellott, R.L. Dunbrack, J.D. Evanseck, M.J. Field, S. Fischer, J. Gao, H. Guo, S. Ha, D. Joseph-McCarthy, L. Kuchnir, K. Kuczera, F.T. Lau, C. Mattos, S. Michnick, T. Ngo, D.T. Nguyen, B. Prodhom, W.E. Reiher, B. Roux, M. Schlenkrich, J.C. Smith, R. Stote, J. Straub, M. Watanabe, J. Wiórkiewicz-Kuczera, D. Yin, M. Karplus, All-atom empirical potential for molecular modelling and dynamics studies of proteins, J. Phys. Chem. B 102 (1998) 3586–3616.
[35] M.P. Johansson, V.R. Kaila, L. Laakkonen, Charge parameterization of the metal centers in cytochrome *c* oxidase, J. Comput. Chem. 29 (2008) 753–767.
[36] T. Darden, D. York, L. Pedersen, Particle mesh Ewald: an $N\cdot\log(N)$ method for Ewald sums in large systems, J. Chem. Phys. 98 (1993) 10089–10092.
[37] W. Humphrey, A. Dalke, K. Schulten, VMD — visual molecular dynamics, J. Mol. Graph. 14 (1996) 33–38.
[38] D. Bashford, K. Gerwert, Electrostatic calculations of the pKa values of ionizable groups in bacteriorhodopsin, J. Mol. Biol. 224 (1992) 473–486.
[39] D. Bashford, An object-oriented programming suite for electrostatic effects in biological molecules an experience report on the MEAD project, Scientific Computing in Object-Oriented Parallel EnvironmentsLecture Notes in Computer Science, 13431997. 233–240.
[40] G. Kieseritzky, E.W. Knapp, Optimizing pKA computation in proteins with pH adapted conformations (PACs), Proteins: Struct. Funct. Bioinf. 71 (2008) 1335–1348.
[41] B. Rabenstein, E.W. Knapp, Calculated pH-dependent population and protonation of carbon-monoxy-myoglobin conformers, Biophys. J. 80 (2001) 1141–1150.
[42] V. Sacks, Y. Marantz, A. Aagaard, S. Checover, E. Nachliel, M. Gutman, The dynamic feature of the proton collecting antenna of a protein surface, Biochim. Biophys. Acta Bioenerg. 1365 (1998) 232–240.
[43] R. Friedman, E. Nachliel, M. Gutman, Application of classical molecular dynamics for evaluation of proton transfer mechanism on a protein, Biochim. Biophys. Acta Bioenerg. 1710 (2005) 67–77.
[44] Y. Marantz, E. Nachliel, A. Aagaard, P. Brzezinski, M. Gutman, The proton collecting function of the inner surface of cytochrome *c* oxidase from *Rhodobacter sphaeroides*, Proc. Natl. Acad. Sci. U. S. A. 95 (1998) 8590–8595.
[45] T. Yamashita, G.A. Voth, Properties of hydrated excess protons near phospholipid bilayers, J. Phys. Chem. B 114 (2010) 592–603.
[46] L. Öjemyr, T. Sandén, J. Widengren, P. Brzezinski, Lateral proton transfer between the membrane and a membrane protein, Biochemistry 48 (2009) 2173–2179.
[47] L. Öjemyr, C. von Ballmoos, K. Faxén, E. Svahn, P. Brzezinski, The membrane modulates internal proton transfer in cytochrome *c* oxidase, Biochemistry 51 (2012) 1092–1100.
[48] M.R. Moncelli, L. Becucci, R. Guidelli, The intrinsic pKa values for phosphatidylcholine, phosphatidylethanolamine, and phosphatidylserine in monolayers deposited on mercury electrodes, Biophys. J. 66 (1994) 1969–1980.
[49] T.H. Haines, N.A. Dencher, Cardiolipin: a proton trap for oxidative phosphorylation, FEBS Lett. 528 (2002) 35–39.
[50] M. Dahlberg, A. Marini, B. Mennucci, A. Maliniak, Quantum chemical modeling of the cardiolipin headgroup, J. Phys. Chem. A 114 (2010) 4375–4387.
[51] K.S. Alnajjar, T. Cvetkov, L. Prochaska, Role of phospholipids of subunit III in the regulation of structural rearrangements in cytochrome *c* oxidase of *Rhodobacter sphaeroides*, Biochemistry 54 (2015) 1053–1063.
[52] M. Wikström, M.I. Verkhovsky, The D-channel of cytochrome oxidase: an alternative view, Biochim. Biophys. Acta Bioenerg. 1807 (2011) 1273–1278.
[53] J.R. Fetter, et al., Possible proton relay pathways in cytochrome c oxidase, Proc. Natl. Acad. Sci. U. S. A. 92 (1995) 1604–1608.
[54] J.W. Thomas, A. Puustinen, J.O. Albern, R.B. Gennis, M. Wikström, Substitution of asparagine for aspartate-135 in subunit I of the cytochorme bo ubiquinol oxidase of *Escherichia coli* eliminates proton-pumping activity, Biochemistry 32 (1993) 10923–10928.